MOX-Report No. 22/2015

Flux form Semi-Lagrangian methods for parabolic problems

Bonaventura, L.; Ferretti, R.

Flux form Semi-Lagrangian methods
for parabolic problems

Luca Bonaventura[1], Roberto Ferretti[2]

May 5, 2015

[1] MOX – Modelling and Scientific Computing,
Dipartimento di Matematica, Politecnico di Milano
Via Bonardi 9, 20133 Milano, Italy
`luca.bonaventura@polimi.it`

[2] Dipartimento di Matematica e Fisica
Università degli Studi Roma Tre
L.go S. Leonardo Murialdo 1, 00146, Roma, Italy
`ferretti@mat.uniroma3.it`

Abstract

A semi-Lagrangian method for parabolic problems is proposed, that extends previous work by the authors to achieve a fully conservative, flux-form discretization of linear and nonlinear diffusion equations. A basic consistency and convergence analysis are proposed. Numerical examples validate the proposed method and display its potential for consistent semi-Lagrangian discretization of advection–diffusion and nonlinear parabolic problems.

1 Introduction.

It is well known that, in their original formulation, Semi-Lagrangian (SL) schemes were developed for the case of purely hyperbolic equations and do not guarantee conservation of mass. In recent years, an increasing number of SL discretization approaches have been proposed to circumvent these limitations.

Various extensions of the SL strategy to second order, parabolic problems, appear for example in [4], [9], [18], [19], [20], [29] (see also [7] for a more complete review), as opposite to the "classical" technique of treating in Eulerian form diffusion terms within SL schemes. In spite of the variety of applications involved, the common feature of these works is to replace the computation of the solution at the foot of a characteristic with a weighted average of values computed at multiple points. A rigorous derivation of these techniques can be based on the Feynman–Kač representation formula, with stochastic trajectories integrated backward in time as in conventional SL schemes. However, due to their stochastic origin, all these generalizations of the SL approach are based on the trace form of parabolic problems, and unsuitable for the divergence form

$$u_t = \operatorname{div}(D\nabla u) \tag{1}$$

which is the most widely used in many applications, especially those to computational fluid dynamics on geophysical scales, for which SL methods for advective problems have proven to be especially useful (see e.g. the review in [3]). In the previous paper [2], we have proposed for the first time a SL method for parabolic problems in divergence form. Numerical experiments reported therein show that the method, albeit formally only first-order accurate in time, allows to compute remarkably accurate approximations of linear and nonlinear parabolic problems, as well as to achieve easily higher order accuracy in space also on nonuniform meshes.

On the other hand, the last two decades have witnessed an increasing interest in conservative, flux-form SL (FFSL) schemes which have been proposed, e.g., in [21], [11], [13], [15], [23], [24], [25], [27], [28], for various linear and nonlinear advective problems. These methods are exactly mass conservative, as opposed to methods based on upstream remapping of computational cells (also called inherently conservative in the literature), see e.g. [5], [6], [12], [14], [16], [17], [22], [26], [31], [32], [33], [34].

The method proposed in [2], however, even though discretizing Equation (1) directly, is not formulated in flux form at the discrete level and does not guarantee exact mass conservation. In the present

work, we try to fill the gap by extending the approach of [2] to achieve a fully conservative, flux form discretization of the diffusion equation (1). Along the same lines as [2], we outline a consistency and stability analysis of the method in a simplified setting, and perform a number of numerical simulations to validate the proposed method.

The paper is structured as follows. In Section 2, our novel FFSL discretization is introduced, while an analysis of its consistency and stability properties will be presented in Sections 3 and 4. Section 5 treats the extensions of the scheme to problems in higher dimensions. Finally, numerical results obtained with the proposed method for both linear and nonlinear models will be presented in Section 6, while some conclusions on the potential advantages of our approach will be drawn in Section 7.

2 Flux Form Semi-Lagrangian methods for second order problems.

In order to sketch the basic ideas of the scheme, we restrict for the moment to the approximation of the pure diffusion equation

$$u_t = (\nu(x,t)u_x)_x \qquad (2)$$

in a single space dimension, considered for simplicity on the whole real line. The extension to advection–diffusion equations and to multiple dimensions will be discussed later in this Section and in Section 5. We have shown in [2] that (2) can be approximated via an abstract difference operator in the form of a convex combination of pointwise values. More specifically, let Δt and Δx denote the time and space discretization steps, respectively, with $t_n = n\Delta t$ for $n \in [0, T/\Delta t]$. The space grid is supposed to be infinite and uniform, that is, for $i \in \mathbb{Z}$, $x_i = i\Delta x$. In the case of the conservative scheme, we will also consider the intermediate points $x_{i\pm 1/2} = (i \pm 1/2)\Delta x$, which will appear as endpoints of grid cells $\Omega_i = [x_{i-1/2}, x_{i+1/2}]$. The nonconservative method is derived by setting

$$u(x_i, t_{n+1}) \approx A_i^+ u(x_i + \delta_i^+, t_n) + A_i^- u(x_i - \delta_i^-, t_n), \qquad (3)$$

provided the constants A_i^+, A_i^-, δ_i^+, δ_i^+ satisfy the consistency conditions

$$\begin{cases} A_i^+ + A_i^- = 1 + O(\Delta t^2) \\ A_i^+ \delta_i^+ - A_i^- \delta_i^- = \Delta t\, \nu_x + O(\Delta t^2) \\ A_i^+ \delta_i^{+2} + A_i^- \delta_i^{-2} = 2\Delta t\, \nu + O(\Delta t^2) \\ A_i^+ \delta_i^{+3} - A_i^- \delta_i^{-3} = O(\Delta t^2). \end{cases} \qquad (4)$$

4

Note that, actually, the additional condition $\delta_i^{\pm 4} = O(\Delta t^2)$ should also be added, which is however already implied by the second condition. We will denote the numerical solutions at time t_n by the vector $V^n = (v_i^n)_{i \in \mathbb{Z}}$. While in the nonconservative form SL scheme these values should be understood as pointwise values, in a FFSL scheme they must be interpreted as cell averages.

In [2], the abstract structure introduced in (4) takes the specific form of the nonconservative approximation

$$v_i^{n+1} = \frac{1}{2}I_p[V^n](x_i + \delta_i^+) + \frac{1}{2}I_p[V^n](x_i - \delta_i^-), \tag{5}$$

where the pointwise values are reconstructed by the interpolation operator (of degree p) $I_p[V^n]$, while the displacements $\delta_i^\pm$ are given as solution of the equation

$$\delta_i^\pm = \sqrt{2\Delta t\, \nu(x_i \pm \delta_i^\pm, t^n)}. \tag{6}$$

For a flux form variant of the above approach, rather than approximating a pointwise value, the cell averages

$$\bar{u}_i(t) \approx \frac{1}{\Delta x}\int_{\Omega_i} u(x,t)dx$$

of the solutions of Equation (2) must be approximated, as customary in finite volume methods, to obtain the discrete mass balance

$$\bar{u}_i(t_{n+1}) \approx \bar{u}_i(t_n) + \frac{1}{\Delta x}\left(\mathcal{F}_{i+1/2}^n - \mathcal{F}_{i-1/2}^n\right). \tag{7}$$

The flux $\mathcal{F}_k^n$ might be defined in abstract form as

$$\mathcal{F}_k^n = \frac{1}{2}\left(\int_{x_k}^{x_k+\delta_k} u(x,t_n)dx - \int_{x_k-\delta_k}^{x_k} u(x,t_n)dx\right)$$

for a properly defined δ_k. The practical version of the scheme implements this operator with a numerically reconstructed function, so that the proposed FFSL method for Equation (2) is defined as

$$v_i^{n+1} = v_i^n + \frac{1}{\Delta x}\left(F_{i+1/2}^n - F_{i-1/2}^n\right) \tag{8}$$

with a numerical flux given, for $k = i \pm 1/2$, by

$$F_k^n = \frac{1}{2}\left(\int_{x_k}^{x_k+\delta_k} R_q[V^n](x)dx - \int_{x_k-\delta_k}^{x_k} R_q[V^n](x)dx\right), \tag{9}$$

and with

$$\delta_k = \sqrt{2\Delta t\, \nu(x_k, t^n)}. \tag{10}$$

Here, the operator $R_q[V]$ is a polynomial reconstruction of degree q which satisfies over each cell $\Omega_m = [x_{m-1/2}, x_{m+1/2}]$ the properties of having the correct cell average w_m and reconstructing with order $O(\Delta x^{q+1})$ a smooth solution. There is a close relationship between the two operators I_p and R_q. We refer to [10] for an in-depth discussion of these theoretical issues, while in Section 4 will recall the main points of interest for the purpose of a stability analysis of the proposed method. It should be remarked that, in this case, it is not required to solve any equation to obtain δ_k. Furthermore, notice that both methods (5) and (8) employ viscosity values frozen at the time level t_n, so that an extension to the nonlinear case is straightforward.

In order to provide a more intuitive interpretation of the proposed scheme, it could be observed that the effect of diffusion (as modeled by Fick's law implicit in Equation (2)) is to move mass from regions with high density towards regions with low density. The difference of integrals in (9) can be shown to be an approximate model of this process. Indeed, the interval $\sqrt{2\Delta t\,\nu}$ is the correct space scale associated to the given diffusion over a time step Δt. Furthermore, it can be observed that

$$\int_{x_k}^{x_k+\delta_k} u(x, t_n)dx \approx \delta_k\, u\left(x_k + \frac{\delta_k}{2}, t_n\right),$$

$$\int_{x_k-\delta_k}^{x_k} u(x, t_n)dx \approx \delta_k\, u\left(x_k - \frac{\delta_k}{2}, t_n\right),$$

so that, as a consequence, one obtains

$$\begin{aligned}
\mathcal{F}_k^n &\approx \frac{\delta_k}{2}\left(u\left(x_k + \frac{\delta_k}{2}, t_n\right) - u\left(x_k - \frac{\delta_k}{2}, t_n\right)\right) \approx \\
&\approx \frac{\delta_k^2}{2}\, u_x(x_k, t_n) = \Delta t\,\nu(x_k, t^n)\, u_x(x_k, t_n)
\end{aligned}$$

which clearly makes (7) consistent with (2). Of course, this is rather a heuristic explanation than a rigorous consistency analysis. Consistency (and its optimal rate) will be proven in the next Section on the basis of conditions (4).

We now show briefly how the proposed FFSL method can be combined with analogous methods for the flux form advection equation. Consider the advection-diffusion equation

$$u_t + (f(x, t)u)_x = (\nu(x, t)u_x)_x, \tag{11}$$

taken again for simplicity on the infinite real line. The combination of the FFSL methods for advection and diffusion is obtained, for the purposes of this paper, by a simple operator splitting approach. This

combination results in a method that is first order accurate in time, which is compatible with the time accuracy of the FFSL method for diffusion, as it will be seen in Section 3. In a first step, any FFSL method for advection can be used. In Section 6, we consider for concreteness the well-known method presented in [15]. This results in a numerical approximation of the cell averages $\tilde{v}_i^{n+1}$ of the solution of (11) with $\nu = 0$. An approximation of the solution of the complete Equation (11) is then obtained by computation of formula (8) based on the intermediate values $\tilde{v}_i^{n+1}$.

3 Consistency.

To prove consistency of the flux form SL method, we start by neglecting the error associated to the space discretization and rewriting the right-hand side of (7) in the more convenient form:

$$
\begin{aligned}
\bar{u}_i(t_n) + \frac{1}{\Delta x}\left(\mathcal{F}_{i+1/2}^n - \mathcal{F}_{i-1/2}^n\right) &= \bar{u}_i(t_n) + \frac{1}{2\Delta x}\left(\int_{x_{i+1/2}}^{x_{i+1/2}+\delta_{i+1/2}} - \int_{x_{i+1/2}-\delta_{i+1/2}}^{x_{i+1/2}} - \right. \\
&\qquad \left. - \int_{x_{i-1/2}}^{x_{i-1/2}+\delta_{i-1/2}} + \int_{x_{i-1/2}-\delta_{i-1/2}}^{x_{i-1/2}}\right) u(x,t_n)dx = \\
&= \bar{u}_i(t_n) + \frac{1}{2\Delta x}\left(\int_{x_{i-1/2}-\delta_{i-1/2}}^{x_{i+1/2}-\delta_{i+1/2}} - \int_{x_{i-1/2}}^{x_{i+1/2}} + \right. \\
&\qquad \left. + \int_{x_{i-1/2}+\delta_{i-1/2}}^{x_{i+1/2}+\delta_{i+1/2}} - \int_{x_{i-1/2}}^{x_{i+1/2}}\right) u(x,t_n)dx.
\end{aligned}
$$

We obtain therefore

$$
\bar{u}_i(t_n) + \frac{1}{\Delta x}\left(\mathcal{F}_{i+1/2}^n - \mathcal{F}_{i-1/2}^n\right) = \frac{1}{2\Delta x}\left(\int_{x_{i-1/2}-\delta_{i-1/2}}^{x_{i+1/2}-\delta_{i+1/2}} + \int_{x_{i-1/2}+\delta_{i-1/2}}^{x_{i+1/2}+\delta_{i+1/2}}\right) u(x,t_n)dx.
\tag{12}
$$

The terms $\delta_{i\pm1/2}$ can also be expressed as

$$
\begin{aligned}
\delta_{i\pm1/2} &= \sqrt{2\Delta t\,\nu(x_{i\pm1/2})} = \tag{13} \\
&= \sqrt{2\Delta t\left(\nu \pm \frac{\Delta x}{2}\nu_x + \frac{\Delta x^2}{8}\nu_{xx} + O\left(\Delta x^3\right)\right)} = \\
&= \sqrt{2\Delta t\,\nu\left(1 \pm \frac{\Delta x\,\nu_x}{2\nu} + \frac{\Delta x^2\,\nu_{xx}}{8\nu} + O\left(\Delta x^3\right)\right)} = \\
&= \delta_i\left(1 \pm \frac{\Delta x\,\nu_x}{4\nu} + \frac{\Delta x^2}{16\nu}\left(\nu_{xx} - \frac{\nu_x^2}{2\nu^2}\right) + O\left(\Delta x^3\right)\right),
\end{aligned}
$$

7

where, in the last row, we have applied the Taylor expansion of the square root and collected all terms of order $O(\Delta x^3)$. It is now easy to recognize that, once replaced (up to a $O(\Delta x^2)$ error) the integrals in the last row of (12) with their midpoint approximation, i.e.,

$$\int_{x_{i-1/2}\pm\delta_{i-1/2}}^{x_{i+1/2}\pm\delta_{i+1/2}} u(x,t_n)dx = (\Delta x \pm \delta_{i+1/2} \mp \delta_{i-1/2})u(x_i \pm \delta_i) + O\left(\Delta x^2\right),$$

and using (13), then (12) is in the form (3), with

$$\delta_i^\pm = \delta_i \tag{14}$$

$$A_i^\pm = \frac{\Delta x \pm (\delta_{i+1/2} - \delta_{i-1/2})}{2\Delta x} = \tag{15}$$

$$= \frac{1}{2} \pm \frac{\delta_i \nu_x}{4\nu} + O\left(\Delta x^2\right).$$

We check now that (14)– (16) satisfy the consistency conditions (4). The first condition is clearly satisfied. As for the second, we have

$$A_i^+ \delta_i^+ - A_i^- \delta_i^- = \delta_i\left(A_i^+ - A_i^-\right) =$$
$$= \frac{\delta_i^2 \nu_x}{2\nu} + O\left(\Delta x^2\right) =$$
$$= \Delta t\, \nu_x + O\left(\Delta x^2\right).$$

The third condition is rewritten as

$$A_i^+ \delta_i^{+2} + A_i^- \delta_i^{-2} = \delta_i^2\left(A_i^+ + A_i^-\right) =$$
$$= 2\Delta t\, \nu\left(1 + O\left(\Delta x^2\right)\right).$$

Finally, for the fourth condition we obtain

$$A_i^+ \delta_i^{+3} - A_i^- \delta_i^{-3} = (2\Delta t\, \nu)^{3/2}\left(\frac{\delta_i \nu_x}{2\nu} + O\left(\Delta x^2\right)\right) =$$
$$= O\left(\Delta t^2\right),$$

in which the last expression is achieved by taking into account that

$$\frac{\delta_i \nu_x}{2\nu} = O\left(\Delta t^{1/2}\right).$$

Therefore, the abstract operator is consistent. Finally, introducing the polynomial reconstruction $R_q[V]$, we note that fluxes are approximated with accuracy of order $O(\Delta x^{q+2})$. Then, the estimate

$$L(\Delta x, \Delta t) = O\left(\Delta t^r + \frac{\Delta x^s}{\Delta t}\right), \tag{16}$$

holds for the truncation error L, with $r = 1$ and $s = q + 2$.

4 Stability.

We briefly discuss the stability of the proposed scheme in the case of a constant coefficient equations, while variable coefficient equations seem to require a deeper study. First, we note that a well understood case is the construction of the nonconservative scheme with I_p in the form of a symmetric Lagrange interpolation, for p odd. For example, if $p = 3$, the value $I_3[V](x)$ is computed, for $x \in [x_k, x_{k+1}]$, by interpolating the values $v_{k-1}, \ldots, v_{k+2}$. In the pure advection case, this construction is known to be stable (see [8]). In order to construct a stable conservative scheme, we can define the reconstruction R_q (see [10] for more details and examples) according to the axioms

i) For $x \in \Omega_m$, $R_q[W](x) = Q_m(x)$ for some polynomial $Q_m \in \mathbb{P}_q$, with q even;

ii) For $x \in \Omega_m$, $Q_m(x)$ depends on the values w_k, with $k = m - q/2, \ldots, m + q/2$, and more precisely it satisfies the conditions

$$\frac{1}{\Delta x} \int_{\Omega_k} Q_m(x)dx = w_k \qquad (k = m - q/2, \ldots, m + q/2).$$

With this definition, it is proven in [10] that, if $p = q + 1$, then

$$\frac{1}{\Delta x} \int_{x-\Delta x/2}^{x+\Delta x/2} R_q[W](\xi)d\xi = I_p[W](x). \tag{17}$$

Consider now the problem (2) for a constant diffusivity ν. In this case $\delta_i \equiv \delta$, so that, rewriting (12) for the reconstructed numerical solution and using (17), we get

$$
\begin{aligned}
v_i^{n+1} &= v_i^n + \frac{1}{\Delta x}\left(F_{i+1/2}^n - F_{i-1/2}^n\right) = \tag{18}\\
&= \frac{1}{2}\left(\frac{1}{\Delta x}\int_{x_{i-1/2}-\delta}^{x_{i+1/2}-\delta} + \frac{1}{\Delta x}\int_{x_{i-1/2}+\delta}^{x_{i+1/2}+\delta}\right)R_q[V^n](x)dx = \\
&= \frac{1}{2}I_p[V^n](x-\delta) + \frac{1}{2}I_p[V^n](x+\delta).
\end{aligned}
$$

The scheme can then be recast as the convex combination

$$V^{n+1} = \frac{1}{2}B^+V^n + \frac{1}{2}B^-V^n, \tag{19}$$

where the terms $B^{\pm}V^n$ represent respectively the schemes written in extended form as

$$v_i^{n+1} = I_p[V^n](x_i \pm \delta),$$

which (see [8]) are stable in the 2-norm for any δ and p. This implies that

$$\left\| B^\pm \right\|_2 \leq 1,$$

and therefore that the complete scheme is also stable in the same norm.

5   Multiple space dimensions.

In this Section, we discuss the extension of the proposed approach to the d-dimensional case. The extension is straightforward in the case of a structured orthogonal grid and diagonal diffusivity matrix

$$\Lambda(x,t) = \text{diag}(\nu_1(x,t), \ldots, \nu_d(x,t)), \tag{20}$$

and in particular, for a variable but isotropic diffusion (for which $\nu_1(x,t) = \cdots = \nu_d(x,t)$). Then, the diffusion equation reads

$$\begin{aligned} u_t &= \text{div}(\Lambda(x,t)\nabla u) = \\ &= \sum_{j=1}^{d}(\nu_j(x,t)u_{x_j})_{x_j}. \end{aligned}$$

By a first-order expansion of the solution with respect to time, we get

$$\begin{aligned} u(x,t+\Delta t) &= u(x,t) + \Delta t \sum_{j=1}^{d}(\nu_j u_{x_j})_{x_j}(x,t) + O(\Delta t^2) = \\ &= \sum_{j=1}^{d}\left[\frac{u(x,t)}{d} + \frac{\Delta t}{d}(d\nu_j u_{x_j})_{x_j}(x,t)\right] + O(\Delta t^2) = \\ &= u(x,t) + \frac{1}{d}\sum_{j=1}^{d}\left[\Delta t(d\nu_j u_{x_j})_{x_j}(x,t)\right] + O(\Delta t^2), \end{aligned}$$

which shows that, up to first-order accuracy, the d-dimensional version can be obtained by averaging the diffusion operators in each direction, with the only modification of scaling each one-dimensional diffusivity by a factor d. This allows to split the diffusion along each of the variables, where (in case of an orthogonal mesh) flux tubes are also aligned with the grid.

For example, the 2-dimensional equation

$$u_t = (\nu_1(x,t)u_{x_1})_{x_1} + (\nu_2(x,t)u_{x_2})_{x_2}$$

would be approximated by the scheme (written with an obvious notation at the node $x_i = (x_{i_1}, x_{i_2})$)

$$v_i^{n+1} = v_i^n + \frac{1}{\Delta x^2} \left(F_{i_1+1/2,i_2}^n - F_{i_1-1/2,i_2}^n + F_{i_1,i_2+1/2}^n - F_{i_1,i_2+1/2}^n \right),$$

(21)

in which, for example, the flux $F_{i_1+1/2,i_2}^n$ would be given by

$$F_{i_1+1/2,i_2}^n = \frac{1}{4} \left(\int_{x_{i_2-1/2}}^{x_{i_2+1/2}} \int_{x_{i_1+1/2}}^{x_{i_1+1/2}+\delta_{i_1+1/2,i_2}} R[V^n](x)dx - \right.$$ (22)

$$\left. - \int_{x_{i_2-1/2}}^{x_{i_2+1/2}} \int_{x_{i_1+1/2}-\delta_{i_1+1/2,i_2}}^{x_{i_1+1/2}} R[V^n](x)dx \right),$$

and the displacement $\delta_{i_1+1/2,i_2}$ defined, at the centers of E and W facets of a square cell, by

$$\delta_{i_1+1/2,i_2} = \sqrt{4\Delta t\, \nu_1(x_{i_1+1/2,i_2}, t^n)}.$$

Note that the integrals appearing in all the fluxes of the form (22) have an integration domain consisting of a row (or column) of grid cells, among which at most one is intersected.

6   Numerical experiments.

Several numerical experiments have been carried out with simple implementations of the FFSL method proposed above, in order to assess its accuracy and stability features also in cases more complex than those allowing a complete theoretical analysis. The accuracy of the proposed discretization has been evaluated against analytic solutions or reference solutions obtained by alternative discretizations in space and time. Due to the close relationship between the methods proposed here and those in [2], the choice of the test cases follows closely the outline in our previous paper, in order to allow for a clear comparison between the conservative and nonconservative SL discretizations.

6.1   Constant coefficient case.

In a first set of numerical experiments, the constant coefficient diffusion equation

$$u_t = \nu u_{xx} \qquad x \in [0, L]$$

was considered, on an interval $[0, L]$ with $L = 10$. Periodic boundary conditions were assumed and a Gaussian profile centered at $L/2$ was

Resolution			l_2 rel. error (SL)		l_2 rel. error (FFSL)	
N	M	μ	I_1	I_3	R_0	R_2
200	50	0.8	$1.50 \cdot 10^{-2}$	$3.33 \cdot 10^{-4}$	$1.5 \cdot 10^{-2}$	$3.79 \cdot 10^{-4}$
200	100	0.4	$1.45 \cdot 10^{-2}$	$2.91 \cdot 10^{-4}$	$1.45 \cdot 10^{-2}$	$2.02 \cdot 10^{-4}$
200	200	0.2	$6.53 \cdot 10^{-2}$	$5.89 \cdot 10^{-4}$	$6.53 \cdot 10^{-2}$	$2.28 \cdot 10^{-4}$
400	100	1.6	$6.53 \cdot 10^{-3}$	$1.92 \cdot 10^{-4}$	$6.53 \cdot 10^{-3}$	$1.78 \cdot 10^{-4}$
400	200	0.8	$1.48 \cdot 10^{-2}$	$8.29 \cdot 10^{-5}$	$1.48 \cdot 10^{-2}$	$9.45 \cdot 10^{-5}$
400	400	0.4	$1.43 \cdot 10^{-2}$	$7.43 \cdot 10^{-5}$	$1.43 \cdot 10^{-2}$	$5.03 \cdot 10^{-5}$

Table 1: Relative errors for the constant coefficient pure diffusion case in the l_2-norm, nonconservative (SL) and conservative (FFSL) scheme, first and third order space discretizations.

considered as the initial condition. In this case, the exact solution can be computed up to machine accuracy by separation of variables and computation of its Fourier coefficients on a discrete mesh of N points with spacing $\Delta x = L/N$. We consider the FFSL method described in the previous Sections on a time interval $[0, T]$ with $T = 2$, with time steps defined as $\Delta t = T/M$. The stability parameter of standard explicit discretizations of the diffusion operator is defined as $\mu = \nu \Delta t / \Delta x^2$. We consider the case with $\nu = 0.05$ first, whose relative errors are reported in Tables 1-2, as computed in the l_2 and l_∞, respectively. The parallel results for the advection diffusion case

$$u_t + a u_x = \nu u_{xx} \qquad x \in [0, L]$$

with $a = 1.5, \nu = 0.05$ are reported in Tables 3-4, respectively. In this case, the Courant number is defined as $C = a \Delta t / \Delta x$ and the advective flux was computed using either linear or quadratic reconstruction, along the lines of the well known method [15]. The fractional flux employed yields in the low Courant number case a discretization that is equivalent to a flux form Lax-Wendroff method.

It can be observed that, in the linear case, the errors obtained by the SL and FFSL methods are in general of the same order of magnitude, with consistently smaller values for the conservative variant. The slightly larger errors of the FFSL case in the advection diffusion cases are partly explained by the fact that, in the present implementation, for simplicity a second order reconstruction was employed for the advective terms, compared to the third order accurate reconstruction employed for the diffusion terms.

Resolution			l_∞ rel. error (SL)		l_∞ rel. error (FFSL)	
N	M	μ	I_1	I_3	R_0	R_2
200	50	0.8	$1.73 \cdot 10^{-2}$	$3.75 \cdot 10^{-4}$	$1.73 \cdot 10^{-2}$	$4.44 \cdot 10^{-4}$
200	100	0.4	$1.67 \cdot 10^{-2}$	$6.46 \cdot 10^{-4}$	$1.67 \cdot 10^{-2}$	$2.36 \cdot 10^{-4}$
200	200	0.2	$7.41 \cdot 10^{-2}$	$1.63 \cdot 10^{-3}$	$7.41 \cdot 10^{-2}$	$2.67 \cdot 10^{-4}$
400	100	1.6	$7.56 \cdot 10^{-3}$	$2.85 \cdot 10^{-4}$	$7.56 \cdot 10^{-3}$	$2.08 \cdot 10^{-4}$
400	200	0.8	$1.71 \cdot 10^{-2}$	$8.86 \cdot 10^{-5}$	$1.70 \cdot 10^{-2}$	$1.11 \cdot 10^{-4}$
400	400	0.4	$1.65 \cdot 10^{-2}$	$1.94 \cdot 10^{-4}$	$1.65 \cdot 10^{-2}$	$5.89 \cdot 10^{-5}$

Table 2: Relative errors for the constant coefficient pure diffusion case in the l_∞-norm, nonconservative (SL) and conservative (FFSL) scheme, first and third order space discretizations.

Resolution				l_2 rel. error (SL)		l_2 rel. error (FFSL)	
N	M	C	μ	I_1	I_3	R_0	R_2
200	50	1.2	0.8	$1.21 \cdot 10^{-2}$	$3.77 \cdot 10^{-4}$	$2.67 \cdot 10^{-2}$	$6.46 \cdot 10^{-4}$
200	100	0.6	0.4	$3.38 \cdot 10^{-2}$	$2.91 \cdot 10^{-4}$	$4.83 \cdot 10^{-2}$	$1.89 \cdot 10^{-3}$
200	200	0.3	0.2	$4.15 \cdot 10^{-2}$	$1.57 \cdot 10^{-3}$	$1.11 \cdot 10^{-1}$	$2.67 \cdot 10^{-3}$
400	100	1.2	1.6	$5.02 \cdot 10^{-3}$	$1.84 \cdot 10^{-4}$	$1.25 \cdot 10^{-2}$	$2.14 \cdot 10^{-4}$
400	200	0.6	0.8	$1.30 \cdot 10^{-2}$	$1.16 \cdot 10^{-4}$	$3.21 \cdot 10^{-2}$	$4.79 \cdot 10^{-4}$
400	400	0.3	0.4	$2.95 \cdot 10^{-2}$	$4.27 \cdot 10^{-4}$	$4.41 \cdot 10^{-2}$	$6.67 \cdot 10^{-4}$

Table 3: Relative errors for the constant coefficient advection diffusion case in the l_2-norm, nonconservative (SL) and conservative (FFSL) scheme, first and third order space discretizations.

Resolution				l_∞ rel. error (SL)		l_∞ rel. error (FFSL)	
N	M	C	μ	I_1	I_3	R_0	R_2
200	50	1.2	0.8	$1.39 \cdot 10^{-2}$	$4.85 \cdot 10^{-4}$	$3.05 \cdot 10^{-2}$	$6.06 \cdot 10^{-4}$
200	100	0.6	0.4	$3.87 \cdot 10^{-2}$	$2.91 \cdot 10^{-4}$	$5.50 \cdot 10^{-2}$	$1.91 \cdot 10^{-3}$
200	200	0.3	0.2	$4.73 \cdot 10^{-2}$	$1.71 \cdot 10^{-3}$	$1.28 \cdot 10^{-1}$	$2.69 \cdot 10^{-3}$
400	100	1.2	1.6	$5.82 \cdot 10^{-3}$	$2.56 \cdot 10^{-4}$	$1.45 \cdot 10^{-2}$	$2.39 \cdot 10^{-4}$
400	200	0.6	0.8	$1.49 \cdot 10^{-2}$	$2.51 \cdot 10^{-4}$	$3.68 \cdot 10^{-2}$	$4.85 \cdot 10^{-4}$
400	400	0.3	0.4	$3.38 \cdot 10^{-2}$	$4.81 \cdot 10^{-4}$	$5.03 \cdot 10^{-2}$	$6.73 \cdot 10^{-4}$

Table 4: Relative errors for the constant coefficient advection diffusion case in the l_∞-norm, nonconservative (SL) and conservative (FFSL) scheme, first and third order space discretizations.

Resolution			l_2 rel. error (SL)		l_2 rel. error (FFSL)	
N	M	μ	I_1	I_3	R_0	R_2
50	50	0.1	$1.34 \cdot 10^{-1}$	$1.10 \cdot 10^{-3}$	$1.30 \cdot 10^{-1}$	$7.31 \cdot 10^{-3}$
100	25	0.8	$2.10 \cdot 10^{-2}$	$5.74 \cdot 10^{-3}$	$2.10 \cdot 10^{-2}$	$4.75 \cdot 10^{-3}$
100	100	0.2	$7.26 \cdot 10^{-2}$	$4.21 \cdot 10^{-3}$	$7.21 \cdot 10^{-2}$	$3.52 \cdot 10^{-3}$
200	50	1.6	$1.02 \cdot 10^{-2}$	$4.68 \cdot 10^{-3}$	$9.57 \cdot 10^{-3}$	$3.00 \cdot 10^{-3}$

Table 5: Relative errors for the variable coefficient pure diffusion case in the l_2-norm, nonconservative (SL) and conservative (FFSL) scheme, first and third order space discretizations.

6.2 Linear diffusion with variable coefficients.

The diffusion equation

$$u_t = (\nu(x,t)u_x)_x \qquad x \in [0,L]$$

was then considered on a space interval $[0,L]$ and time interval $[0,T]$ with $L = 10$ and with $T = 4$, with time steps defined as $\Delta t = T/M$. Periodic boundary conditions were assumed and a Gaussian profile centered at $L/5$ was considered as the initial condition. The diffusivity field was given by

$$\nu(x,t) = \frac{1}{20} + \frac{1}{5}\xi(x)\sin\left(\frac{2\pi t}{T}\right)^2,$$

respectively, where $\xi(x)$ denotes the characteristic function of the interval $[0.5L, 0.8L]$. This choice highlights the possibility to use the proposed method seamlessly also with strongly varying diffusion coefficients. In this case, no exact solution is available and reference solutions were computed using the finite difference method described in the previous section with a four times higher spatial resolution, coupled to a high order multistep stiff solver in which a small tolerance and maximum time step value were enforced. A plot of the numerical solutions obtained at the final time T are displayed in Figures 1-2, for the FFSL and SL method, respectively.

A more quantitative assessment of the FFSL solution accuracy can be gathered from Tables 5- 6. It can be observed that the FFSL method is always of slightly higher accuracy than the corresponding SL variant at equivalent resolution. In all these computations, FFSL maintains mass conservation up to machine accuracy by construction, while the average conservation error of the SL method is of the order of 10^{-3} of the total initial mass.

Resolution			l_2 rel. error (SL)		l_2 rel. error (FFSL)	
N	M	μ	I_1	I_3	R_0	R_2
50	50	0.1	$1.50 \cdot 10^{-1}$	$1.50 \cdot 10^{-2}$	$1.47 \cdot 10^{-1}$	$1.28 \cdot 10^{-2}$
100	25	0.8	$2.72 \cdot 10^{-2}$	$7.97 \cdot 10^{-3}$	$2.77 \cdot 10^{-2}$	$8.21 \cdot 10^{-3}$
100	100	0.2	$8.78 \cdot 10^{-2}$	$7.42 \cdot 10^{-3}$	$8.87 \cdot 10^{-2}$	$6.71 \cdot 10^{-3}$
200	50	1.6	$1.36 \cdot 10^{-2}$	$6.95 \cdot 10^{-3}$	$1.43 \cdot 10^{-2}$	$5.60 \cdot 10^{-3}$

Table 6: Relative errors for the variable coefficient pure diffusion case in the l_∞-norm, nonconservative (SL) and conservative (FFSL) scheme, first and third order space discretizations.

6.3 Gas flow in porous media.

We reconsider the nonlinear example, already treated in [2], of the one-dimensional equation of gases in porous media,

$$u_t = \left(mu^{m-1}u_x\right)_x, \tag{23}$$

focusing in particular on the so-called Barenblatt–Pattle self-similar solutions (see, e.g., [1]), which can be written in the form

$$u(x,t) = (t+t_0)^{-k}\left(A^2 - \frac{k(m-1)|x|^2}{2m(t+t_0)^{2k}}\right)_+^{\frac{1}{m-1}} \tag{24}$$

where $t_0 > 0$, A is an arbitrary nonzero constant and $k = 1/(m+1)$. In order to adapt the FFSL scheme to this case, we recall what has been already observed for the nonconservative scheme in [2]: since the solution (and hence, the diffusivity) may have a bounded support, a straightforward extension of (6) in the linearized form

$$\delta_i^{\pm} = \sqrt{2\Delta t\, \nu\left(I[V^n](x_i \pm \delta_i^{\pm})\right)} \tag{25}$$

(where in our case $\nu(u) = mu^{m-1}$) would have multiple solutions for x_i out of the support but in its neighbourhood – to ensure a correct propagation of the solution, $\delta_i^{\pm}$ should be defined as the largest of such values. The same caution should be applied in extending the definition (10). A possible answer in this respect is to compute the $\delta_k^{\pm}$ via (25), then define $\delta_k = (\delta_k^+ + \delta_k^-)/2$, where, of course, x_k is now a cell interface.

Figure 3 compares the exact and approximate evolution of the Barenblatt–Pattle solution for (23), with $m = 3$, $A = 1$ and $t_0 = 1$. Approximate solutions have been computed with the nonconservative (a) and the conservative (b) scheme at $T = 1, 4, 16$ on a mesh composed of 50 nodes with $\Delta t = 0.05$, using respectively cubic interpolation and quadratic reconstruction. Note that the mass conservation

Resolution		l_2 relative error (SL)		l_2 relative error (FFSL)	
N	M	I_1	I_3	R_0	R_2
50	320	0.316	$8.69 \cdot 10^{-2}$	0.270	$2.67 \cdot 10^{-2}$
100	640	0.212	$4.76 \cdot 10^{-2}$	0.156	$1.65 \cdot 10^{-2}$
200	1280	0.171	$4.84 \cdot 10^{-2}$	$9.85 \cdot 10^{-2}$	$1.09 \cdot 10^{-2}$
400	2560	0.135	$4.49 \cdot 10^{-2}$	$6.03 \cdot 10^{-2}$	$2.69 \cdot 10^{-3}$
800	5120	0.107	$3.22 \cdot 10^{-2}$	$3.72 \cdot 10^{-2}$	$2.79 \cdot 10^{-3}$

Table 7: Relative errors for the Barenblatt–Pattle solution in the 2-norm, nonconservative (SL) and conservative (FFSL) scheme, first and third order space discretizations.

constraint apparently improves the accuracy of the scheme, especially for larger simulation times. This behaviour is confirmed, in terms of both absolute accuracy and convergence rate, by Table 7, which shows the numerical errors for the two schemes in the 2-norm, at $T = 16$, under a linear refinement law. SL scheme has been tested with linear (I_1) and cubic (I_3) interpolation, whereas FFSL scheme with piecewise constant (R_0) and piecewise quadratic (R_2) reconstruction.

6.4 Variable coefficient case in two space dimensions.

As a two-dimensional test, we consider the equation

$$u_t = \text{div}(\nu(x)\nabla u)$$

on $\Omega = [-3, 3]^2$ with periodic boundary conditions. The initial condition given by the characteristic function of the square $\Sigma = [-1.5, 1.5]^2$. The isotropic diffusivity ν is given by

$$\nu(x) = e^{-5|x-x_0|^2},$$

where $x_0 = (1.5, -1.5)$. The diffusion is therefore concentrated in a corner on the boundary of the set Σ. The effect of this diffusion is to move mass from the interior of Σ to the exterior, in the neighbourhood of the point x_0. Figure 4 shows the numerical solution along with its level curves at $T = 2$, with a 50×50 space grid, R_0 reconstruction and time step $\Delta t = 0.05$. Note that, despite being conceptually obtained by directional splitting, the two-dimensional scheme (21) does not suffer from anisotropies induced by grid orientation.

7 Conclusions.

We have extended the SL approach of [2] to achieve a fully conservative, flux form discretization for linear and nonlinear parabolic problems. A consistency and stability analysis of the method has also been presented, along with a strategy to couple the FFSL discretizations of advection and diffusion terms. A number of numerical simulations validate the proposed method, showing that it is equivalent in accuracy to its nonconservative variant, while allowing to maintain mass conservation at machine accuracy. The proposed method could represent an important complement to the many conservative, flux-form semi-Lagrangian schemes for advection proposed in the literature. Future developments will focus on the application of the proposed approach to conservation laws with nonlinear parabolic terms, such as e.g. the Richards equation, and to the extension of this technique to high order discontinuous finite elements discretizations such as those proposed in [27], [30].

Acknowledgements.

References

[1] G. I. Barenblatt. On self-similar motions of a compressible fluid in a porous medium. *Akad. Nauk SSSR. Prikl. Mat. Meh*, 16(6):79–6, 1952.

[2] L. Bonaventura and R. Ferretti. Semi-Lagrangian methods for parabolic problems in divergence form. *SIAM Journal of Scientific Computing*, 36:A2458 – A2477, 2014.

[3] L. Bonaventura, R. Redler, and R. Budich. *Earth System Modelling 2: Algorithms, Code Infrastructure and Optimisation.* Springer Verlag, New York, 2012.

[4] M. Camilli and M. Falcone. An approximation scheme for the optimal control of diffusion processes. *M2AN*, 29:97–122, 1995.

[5] J.K. Dukowicz. Conservative rezoning (remapping) for general quadrilateral meshes. *Journal of Computational Physics*, 54:411–424, 1984.

[6] J.K. Dukowicz and J.R. Baumgardner. Incremental remapping as a transport/advection algorithm. *Journal of Computational Physics*, 160:318–335, 2000.

[7] M. Falcone and R. Ferretti. *Semi-Lagrangian Approximation Schemes for Linear and Hamilton–Jacobi Equations*. SIAM, 2013.

[8] R. Ferretti. Equivalence of semi-Lagrangian and Lagrange–Galerkin schemes under constant advection speed. *Journal of Computational Mathematics*, 28:461–473, 2010.

[9] R. Ferretti. A technique for high-order treatment of diffusion terms in semi-Lagrangian schemes. *Communications in Computational Physics*, 8:445–470, 2010.

[10] R. Ferretti. Stability of some generalized Godunov schemes with linear high-order reconstructions. *Journal of Scientific Computing*, 57:213–228, 2013.

[11] P. Frolkovic. Flux-based method of characteristics for contaminant transport in flowing groundwater. *Computing and Visualization in Science*, 5:73–83, 2002.

[12] J.P.R. Laprise and R. Plante. A class of semi-Lagrangian integrated-mass (SLIM) numerical transport algorithms. *Monthly Weather Review*, 123:553–565, 1995.

[13] B.P. Leonard, A.P. Lock, and M.K. MacVean. Conservative explicit unrestricted-time-step multidimensional constancy-preserving advection schemes. *Monthly Weather Review*, 124:2588–2606, November 1996.

[14] L.M. Leslie and R.J. Purser. Three-dimensional mass-conserving semi-Lagrangian scheme employing forward trajectories. *Monthly Weather Review*, 123:2551–2566, 1995.

[15] S.J. Lin and Richard B. Rood. Multidimensional flux-form semi-Lagrangian transport schemes. *Monthly Weather Review*, 124:2046–2070, September 1996.

[16] W.H. Lipscomb and T.D. Ringler. An incremental remapping transport scheme on a spherical geodesic grid. *Monthly Weather Review*, 133:2335–2350, 2005.

[17] B. Machenhauer and M. Olk. The implementation of the semi-implicit scheme in cell-integrated semi-Lagrangian models. *Atmosphere-Ocean*, XXXV(1):103–126, March 1997.

[18] G.N. Milstein. The probability approach to numerical solution of nonlinear parabolic equations. *Numerical Methods for Partial Differential Equations*, 18:490–522, 2002.

[19] G.N. Milstein and M.V. Tretyakov. Numerical algorithms for semilinear parabolic equations with small parameter based on approximation of stochastic equations. *Mathematics of Computation*, 69:237–567, 2000.

[20] G.N. Milstein and M.V. Tretyakov. Numerical solution of the dirichlet problem for nonlinear parabolic equations by a probabilistic approach. *IMA Journal of Numerical Analysis*, 21:887–917, 2001.

[21] E. Sonnendrücker N. Crouseilles, M. Mehrenberger. Conservative semi-Lagrangian schemes for the Vlasov equation. *Journal of Computational Physics*, 229:1927–1953, 2010.

[22] R.D. Nair and B. Machenhauer. The mass-conservative cell-integrated semi-Lagrangian advection scheme on the sphere. *Monthly Weather Review*, 130:649–667, 2002.

[23] T.N. Phillips and A.J. Williams. Conservative semi-Lagrangian finite volume schemes. *Numerical Methods for Partial Differential Equations*, 17:403–425, 2001.

[24] J.M. Qiu and C.W. Shu. Conservative high order semi-Lagrangian finite difference WENO methods for advection in incompressible flow. *Journal of Computational Physics*, 230:863889, 2011.

[25] J.M. Qiu and C.W. Shu. Positivity preserving semi-Lagrangian discontinuous Galerkin formulation: Theoretical analysis and application to the Vlasov-Poisson system. *Journal of Computational Physics*, 230:83868409, 2011.

[26] M. Rancic. An efficient, conservative, monotone remapping for semi-Lagrangian transport algorithms. *Monthly Weather Review*, 123:1213–1217, 1995.

[27] M. Restelli, L. Bonaventura, and R. Sacco. A semi-Lagrangian Discontinuous Galerkin method for scalar advection by incompressible flows. *Journal of Computational Physics*, 216:195–215, 2006.

[28] J.A. Rossmanith and D.C. Seal. A positivity-preserving high-order semi-Lagrangian discontinuous Galerkin scheme for the VlasovPoisson equations. *Journal of Computational Physics*, 230:6203–6232, 2011.

[29] J. Teixeira. Stable schemes for partial differential equations: The one-dimensional diffusion equation. *Journal of Computational Physics*, 153:403–417, 1999.

[30] G. Tumolo, L. Bonaventura, and M. Restelli. A semi-implicit, semi-Lagrangian, $p-$adaptive discontinuous Galerkin method for the shallow water equations. *Journal of Computational Physics*, 232:46–67, 2013.

[31] M. Zerroukat, N. Wood, and A. Staniforth. SLICE: a semi-Lagrangian inherently conserving and efficient scheme for transport problems. *Quarterly Journal of the Royal Meteorological Society*, 128:2801–2820, 2002.

[32] M. Zerroukat, N. Wood, and A. Staniforth. SLICE-S: A semi-Lagrangian inherently conserving and efficient scheme for transport problems on the sphere. *Quarterly Journal of the Royal Meteorological Society*, 130:2649–2664, 2004.

[33] M. Zerroukat, N. Wood, and A. Staniforth. A monotonic and positive-definite filter for a semi-Lagrangian inherently conserving and efficient (SLICE) scheme. *Quarterly Journal of the Royal Meteorological Society*, 131:2923–2936, 2005.

[34] M. Zerroukat, N. Wood, A. Staniforth, A. A. White, and J. Thuburn. An inherently conserving semi-implicit semi-Lagrangian discretisation of the shallow water equation on the sphere. *Quarterly Journal of the Royal Meteorological Society*, 135:1104–1116, 2009.
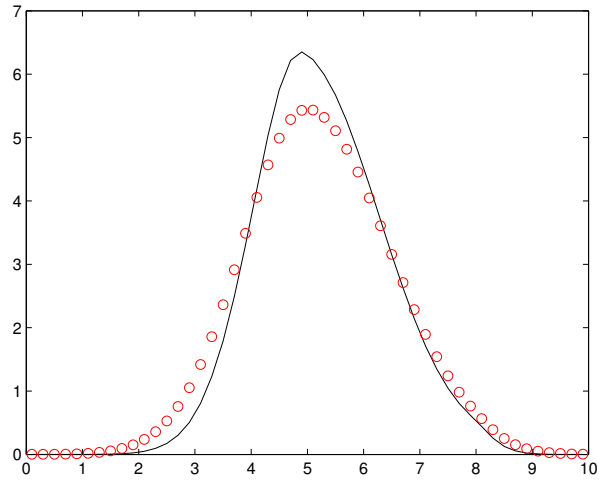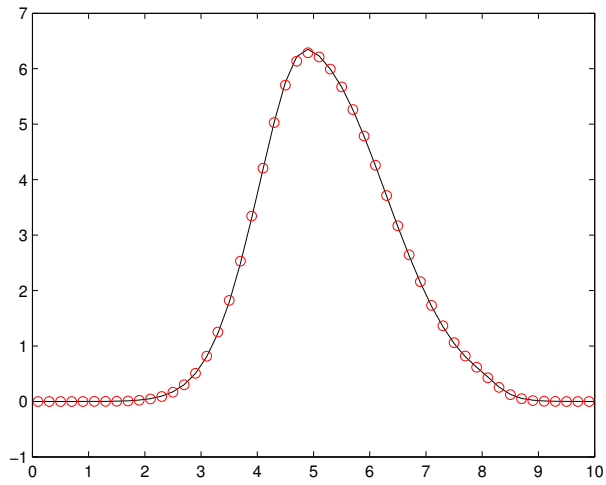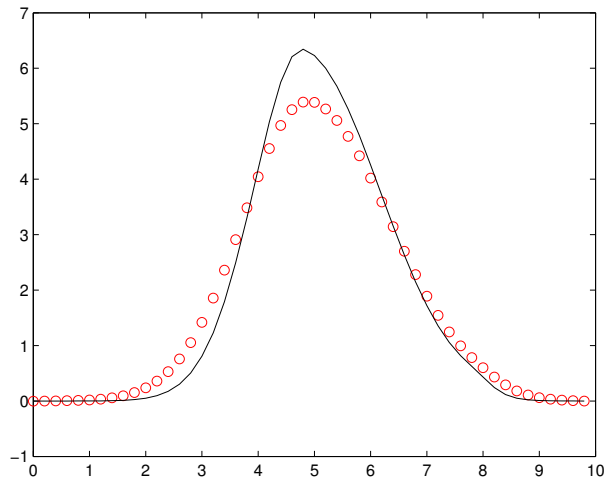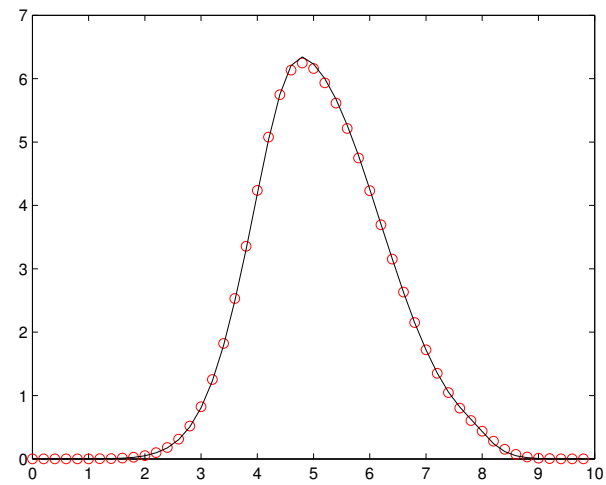
Figure 1: One-dimensional case with variable coefficients: numerical solution by FFSL method with (a) linear (b) cubic reconstruction. Numerical solution is represented by circles, reference solution by continuous line).
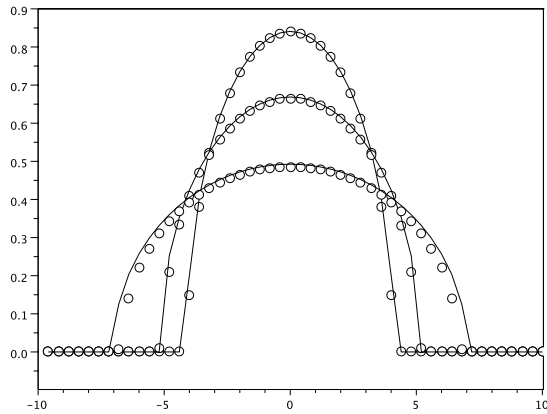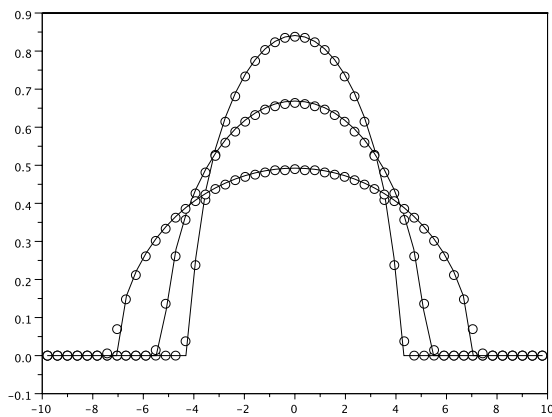
21

Figure 2: One-dimensional case with variable coefficients: numerical solution by SL method with (a) linear (b) cubic reconstruction. Numerical solution is represented by circles, reference solution by continuous line).
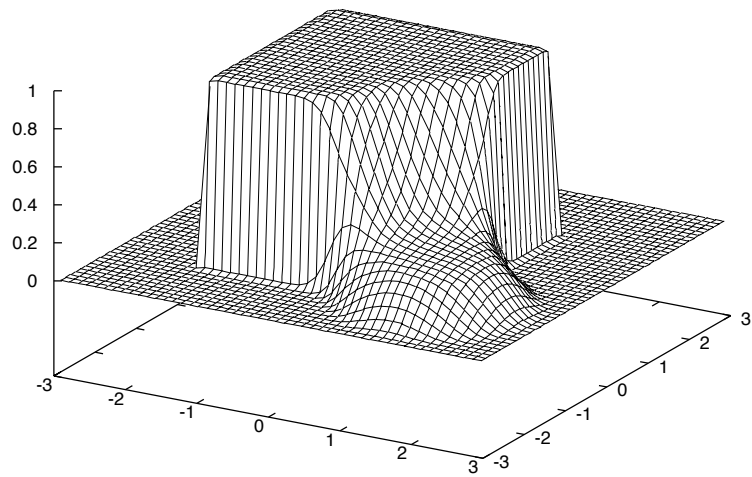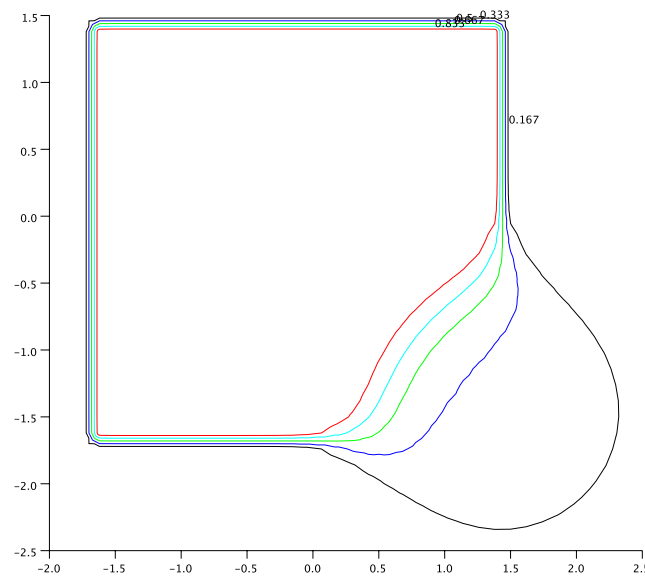
(a)

(b)

Figure 3: Evolution of the exact (continuous line) versus numerical (circles) Barenblatt–Pattle solution for T=1,4,16, nonconservative (a) and conservative (b) scheme.

(a)

(b)

Figure 4: Variable isotropic diffusion, graph (a) and level curves (b) of the solutions.

MOX Technical Reports, last issues

Dipartimento di Matematica
Politecnico di Milano, Via Bonardi 9 - 20133 Milano (Italy)

21/2015 Arena, M.; Azzone, G.; Secchi, P.; Vantini, S.
Reputational risk and corporate finance: A multi-event model

20/2015 Antonietti, P.F.; Formaggia, L.; Scotti, A.; Verani, M.; Verzotti, N.
Mimetic finite difference approximation of flows in fractured porous media

19/2015 Palamara, S.; Lange, M.; Vergara, C.; Lassila, T.; Frangi, A.F.; Quarteroni, A.
A coupled 3D-1D numerical monodomain solver for cardiac electrical activation in the myocardium with detailed Purkinje network

17/2015 Nestola, M.G.C.; Faggiano, E.; Vergara, C.; Lancellotti, R.M.; Ippolito, S,; Filippi, S.; Quarter
Computational comparison of aortic root stresses in presence of stentless and stented aortic valve bio-prostheses

18/2015 Masci, C,; Ieva, F.; Agasisti, T.; Paganoni, A.M.
Bivariate multilevel models for the analysis of mathematics and reading pupils' achievements

16/2015 Fumagalli, I.; Manzoni, A.; Parolini, N.; Verani, M.
Reduced basis approximation and a posteriori error estimates for parametrized elliptic eigenvalue problems

15/2015 Taffetani, M.; de Falco, C.; Penta, R.; Ambrosi, D.; Ciarletta, P.
Biomechanical modelling in nanomedicine: multiscale approaches and future challenges

14/2015 Canuto, C.; Nochetto, R.H.; Stevenson R,; Verani, M.
Convergence and Optimality of hp-AFEM

13/2015 Bartezzaghi, A.; Dedè, L.; Quarteroni, A.;
Isogeometric Analysis of High Order Partial Differential Equations on Surfaces

12/2015 Antonietti, P. F.; Beirao da Veiga, L.; Scacchi, S.; Verani, M.
A C^1 virtual element method for the Cahn-Hilliard equation with polygonal meshes